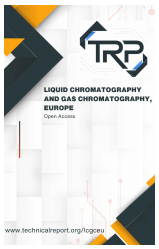

**Journal of Liquid Chromatography and Gas Chromatography, Europe**

https://technicalreport.org/lcgceu/

*LC GC Eu.*, Vol. 37, No.2, 08-15, 2024

Technical Reports Press

RESEARCH ARTICLE

# Terminal-Weighted Carbonate Gating for Intradermal Microneedle Estimation of Blood-Proximal Carbon Dioxide

**Daniel Thompson**[1]

[1]*Department of Environmental Analytical Chemistry Great Lakes University United States*
[*]*Corresponding author*

Corresponding author:
danielthimp@proton.me

**Abstract**

The skin-based transducer used to measure the concentration of CO2 in the skin must generate some chemical response that may be interpreted to form a valid approximation of the blood proximal CO2 concentration. This work introduces the Kernel-Gated Acid-Base Fusion (KG-ABF) carbonate gate for the paired microneedle pH and carbonate data. The key challenge is how the combination of the carbonate filter with the time-weighted animal level fusion impacts the discrepancy between the estimates based on the intradermal readings and the terminal blood-gas $PCO_2$ levels compared with the unfiltered averaged or last microneedle measurement only approach. The analysis dataset consists of six conditioning conditions of the rat skin and twelve animal times from five anesthetized rats. The KG-ABF algorithm assumes the two measurements as a coupled acid-base signal, withholds the blood-proximal CO2 estimation if the measurements of the carbonate, bicarbonate, and transformed $PCO_2$ values are less than useful chemically, and applies weights to the accepted intradermal CO2 values as a function of proximity to the terminal blood sampling. In the full set of ex vivo samples, the intradermal and reference measurements differ by 0.9(5) % for pH, 14.2(28) % for carbonate, and 10.3(97) % for dissolved carbon dioxide. The in vivo gate filtered out one rat 4 sample and accepted eleven animal time measurements from rats 1, 2, 3, and 5. The values for accepted KG-ABF values were 14.7, 53.0, 51.2, and 27.2 mmHg and the reference readings correspondingly equal to 18.8, 48.8, 53.7, and 25.4 mmHg. The achieved mean absolute error amounts to 3.1 mmHg, the root mean squared error equals 3.3 mmHg, and the maximum absolute error is 4.2 mmHg. These results support carbonate-gated interpretation as an essential analytical layer for intradermal gas-sensing patches.

**Keywords:** microneedle sensor; interstitial fluid; carbon dioxide; carbonate chemistry; potentiometric sensing; analytical chemistry; wearable diagnostics; blood-gas comparison.

**Received:** 20 December 2023
**Accepted:** 11 April 2024
**Available online:** 30 June 2024

## 1. Introduction

The level of carbon dioxide serves as a bridge between analytical chemistry and respiratory physiology, since it correlates with breathing parameters, metabolism of tissues, the activity of bicarbonate buffer systems, and acid-base balance. In respiratory distress, anesthesia, intensive care, metabolic abnormalities, and perioperative settings, blood-gas analysis represents the gold standard method for measuring pH, bicarbonate, and $PCO_2$. The level of analytic validity is rather high; however, sampling is invasive, non-continuous, and dependent on the personnel. Continuous arterialization may be inappropriate when carbon dioxide levels change quickly, if blood volumes are limited, or trend data are preferred to spot measurements in a laboratory.

Transcutaneous carbon dioxide measurement methods are less invasive; however, they are prone to calibration, sensor heating, perfusion, motion artifacts, tissue thickness, and environmental effects [1–3]. Capnography provides breath-by-breath data but cannot measure tissue and blood carbon dioxide concentrations due to dead-space effects, ventilation-perfusion mismatch, and local perfusion. In view of these limitations, skin-accessible chemosensing technologies capable of as-

**Cite as:** D. Thompson (2024). Terminal-Weighted Carbonate Gating for Intradermal Microneedle Estimation of Blood-Proximal Carbon Dioxide. LC GC Eu., 37(2) (2024) 08-15.

sessing chemical reactions in the vicinity of the interstitial space have merit.

The dermal interstitial fluid environment is particularly favorable in wearable analytical chemistry, due to its cellular proximity, direct communication with capillary blood, and accessibility using microneedles without causing extensive tissue damage [4, 5]. There is a long history of detecting electrolytes, metabolites, pharmaceuticals, and other small molecules using wearable electrochemistry through the skin [6, 7]. The addition of microneedles confers the key benefit of penetrating the stratum corneum layer and delivering sensor membranes in closer proximity to the dermal environment compared to sweat analysis [8, 9].

Potentiometric microneedles are highly appropriate as an answer to this challenge, due to their ability to monitor the pH and carbonate activity using selective or membrane-based electrodes. Intradermal detection of potassium ions, pH values, and multiple ions has been previously reported with all-solid-state and polymer-based membrane designs [10–12]. Although the devices discussed here are analytical sensors, as opposed to passive collectors, the raw output does not necessarily correspond directly to a blood-gas measurement. Calibration state, useful range, matrix, and chemical interaction should not be overlooked.

CO2 determination requires more stringent conditions than ion determination. Indeed, a single patch may give intradermal pH and carbonate activity, but the comparison variable is typically $PCO_2$. The link between these variables is based on the carbonate acid-base system where dissolved CO2, bicarbonate, carbonate, and hydrogen ions are interconnected. Thus, a pH-carbonate couple does provide CO2 concentration information; however, it is contingent upon assumptions of equilibrium, temperature, ionic strength, selectivity of the membrane electrode, stability of the reference electrode, and local physiological factors [13–15]. Hence, a single transformed value can be numerically precise without being chemically accurate.

The problem of temporal structure is a second issue complicating data analysis. In particular, the in vivo study had intradermal determinations performed before the final sampling of blood gases. Assuming all intradermal samples to be equally relevant for the final blood value overlooks the physiological delay, differences in anesthesia, skin perfusion, and local equilibration. Restricting attention to the last intradermal time point precludes the use of early samples, which are chemically correct, and may put too much weight on local excursions. A more consistent choice would be keeping temporal information while giving priority to the latest reading.

This analysis is not about whether a pH-carbonate microneedle can produce a signal related to carbon dioxide. The challenge is to decide how to transform such a record into an animal-level $PCO_2$ estimate, given that a single animal-time point is chemically deprived, that acceptable readings may vary per animal, and that terminal blood gas measures offer a point of comparison. The algorithm needs to clarify conditions for withholding the estimate, combining repeat measures, and reporting concordance without obscuring the variability associated with intradermal chemistry.

The research question becomes, then: Is there a reduction in error associated with a $PCO_2$ estimate from pairs of intradermal pH-carbonate microneedle records, using a combination of reliability filtering and weight near terminal observation versus averaging or simply accepting the last reading? In answering this question, KG-ABF follows an approach involving two-tiered analytical record, ex vivo verification of the measure, in vivo chemical gating, and animal-level comparison with terminal blood-gas $PCO_2$. The scientific contribution is an explicit chemically-based procedure for reporting estimates, rejections, and variability.

## 2. Materials and Methods

### 2.1. Dataset definition

The analytical data set included microneedle measures of rat skin and anesthetized rats related to intradermal detection of $CO_2$ [16]. In the ex vivo tier, there are six rat skin conditioning states, each including microneedle pH, microneedle carbonate, microneedle dissolved carbon dioxide, and reference data when available. In the in vivo tier, there are twelve animal-time observations from five rats, comprising intradermal pH, carbonate, bicarbonate, dissolved carbon dioxide, and intradermal $PCO_2$, along with blood gas pH, bicarbonate, and $PCO_2$.

No distinct animal preparation, assay, or biological specimen processing took place for this data set. The data were analyzed for analytical validation instead of being used as a clinical data set. The goal was to verify if chemical QC and time-aware data fusion would lead to improvement of the blood proximity of the paired microneedle signals.

### 2.2. Microneedle platform and sampling geometry

As shown in Figures 1, these key components in this device design are: the flexible patch, the elevated microneedle array, the magnified view of the needles, and the cable connection point. These elements are critical to the success of the experiment based on the assumption made by KG-ABF that both channels were derived from the same local intradermal contact area.

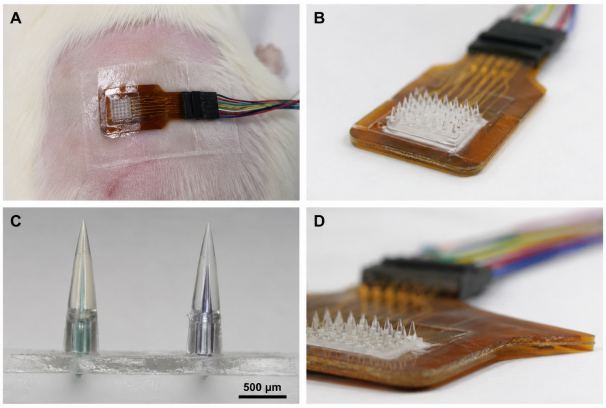


**Figure 1:** Microneedle patch format.

It is evident from the patch design why the analysis requires an assumption about co-location of samples. As long as the patch is kept in stable contact with the elevated microneedles with prepared skin, the paired chemical response channels can be analyzed together instead of as independent readings. In addition, one sees why the quality control step is absolutely required since the cable attachment may give a false impression of stable contact.

Figure 2, depicting the array and skin contact geometries, provides more information about how samples were taken. In terms of the array, it is viewed here as skin facing rather than as a probe inserted into bulk fluid. Hence, one might expect a sampled microenvironment to have finite volume, finite equilibration time, and possibly heterogeneous contact.

Given the geometry above, there is no doubt that time must be considered analytically. In an intradermal microenvironment, the carbonate and pH system can vary as a result of insertion dynamics, hydration, perfusion, metabolism, and equilibration with blood in the body. Therefore, the method does not simply take averages of data for evaluation of chemical suitability.

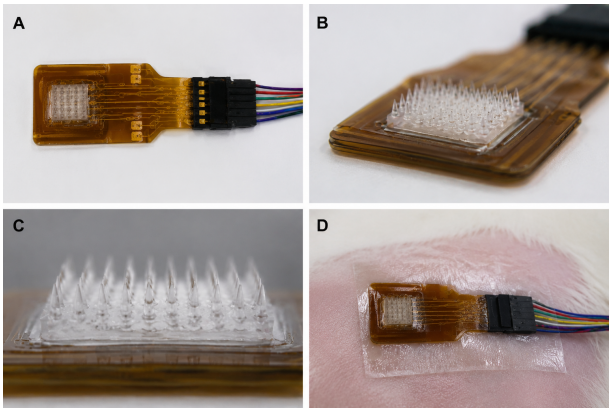


**Figure 2:** Array and skin contact.

### 2.3. Carbonate gating and terminal weighting

The algorithm works through three steps. Firstly, pH and carbonate are considered as a coupled carbonate system reaction rather than as individual responses of the sensors. Secondly, the carbonate reliability gate blocks any use of blood proximal $PCO_2$ when the coupled record has chemical depletion. Thirdly, the fused records in an accepted measure are merged based on how close they were to terminal blood gas analysis.

Only one record would be acceptable when the values of carbonate, bicarbonate, and intradermal $PCO_2$ are equal to or greater than $5\,\mu mol\,L^{-1}$, $10\,mmol\,L^{-1}$, and 10 mmHg respectively. The numbers here do not represent diagnostic criteria and must not be interpreted as biological cutoffs but a useful interval of chemistry operation. When the values are not met by all three criteria, there is a case of coupled depletion pattern that is different from fluctuations of an individual variable.

Records with an acceptable status were weighted using terminal proximity weighting. As the blood-gas sample was taken towards the end of the record-taking procedure, the accepted data taken later had more weight than the accepted data taken earlier. In cases where there were accepted data taken from an animal at 15, 25, and 35 min, the weights were 23.0%, 32.1%, and 44.8% respectively. For the animal with accepted data recorded at 25 and 35 min, the weights were 41.7% and 58.3%. The rationale here is to preserve information from the earlier time but also recognize that the terminal blood comparison is close in time to the final measurement.

For agreement assessment, the mean absolute error, root mean square error, maximum absolute error, and the percentage of accepted animals with an absolute difference of 7.5 mmHg in terminal blood-gas $PCO_2$ were used. Two other approaches for comparison with the KG-ABF approach were unweighted averaging of valid intradermal measurements and taking the last 35 min data.

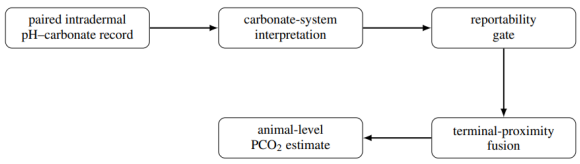


**Figure 3:** KG-ABF workflow.

This workflow allows for the separation of signal generation and analysis steps, which is necessary because a sensible $PCO_2$ estimation and raw transformed value are not one and the same. KG-ABF provides an animal-level value solely based on the application of chemical screening and terminal-time weighting.

## 3. Results and Discussion

### 3.1. Range of the ex vivo response and carbonate accuracy

Testing for chemical sensibility of the paired values at the ex vivo level determines if the range of the measured response in microneedle-pH–carbonate pairs is practical from a skin-contact point of view. Table 1 represents six different conditioned rat skin samples, of which four contain fully obtained data on microneedles and references. In the latter set, the agreement in pH was high, with a difference of only 0.9(5) %. However, the differences were 14.2(28) % and 10.3(97) % for carbonate and carbon dioxide, respectively.

Ex vivo values provide the basis for the carbonate limit in order to determine in vivo acceptability. The pH channel behaved relatively stably throughout the entire comparison group, while carbonate grew increasingly sensitive as conditioning progressed towards low micromolars. Skin 5 is relevant analytically since microneedle carbonate was only slightly different from the reference value at $8.8\,\mu mol\,L^{-1}$ compared to $10.2\,\mu mol\,L^{-1}$; hence, low carbonate levels do not necessarily indicate an invalid record. Skin 6, on the other hand, gave only $2.1\,\mu mol\,L^{-1}$ in microneedle carbonate with incomplete reference validation; hence, this is the threshold at which the validity of carbon dioxide inferences must be questioned.

The ex vivo cell shown in Figure 4 provides proof of the setup performed for skin-contact analysis. The importance of this setup is that a carbonate response at a defined interface is more challenging compared to the same response for a homogeneous bulk sample. The cell provides proof that the paired signal has been measured through proper placement, hence making it an adequate lower-tier verification point.

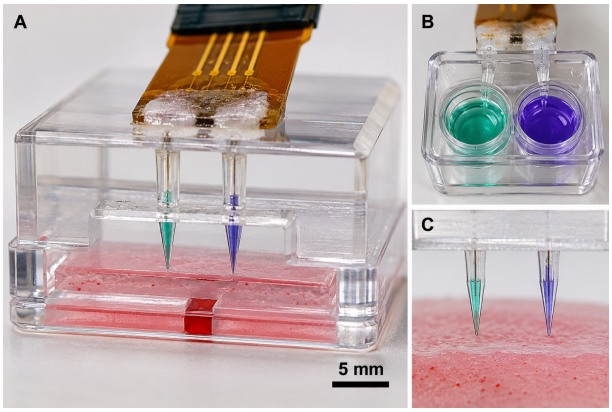


**Figure 4:** Ex vivo test cell.

The contact environment shown in Figure 4 goes some way towards explaining the preference for carbonate analysis as opposed to pH. A pH probe can continue to produce legible output even when carbonate concentration is getting into a region where minor differences in values will result in significant variations in carbon dioxide estimation. This is not a platform issue but highlights the importance of having reliable carbonate levels along with stable pH prior to defining $PCO_2$.

The picture of the chamber in Figure 5 provides physical insight into the interface with skin. The sensor was not being used solely in a detached calibration fluid but was also applied to a defined tissue surface.

The overall meaning of the chamber theory and Table 1 is that rejection should not occur solely due to low pH and/or carbonate levels. Rejec-

**Table 1:** Ex vivo comparison.

| Skin | Conditioning pH | Conditioning $CO_3^{2-}$ ($\mu mol\,L^{-1}$) | MN pH | MN $CO_3^{2-}$ ($\mu mol\,L^{-1}$) | MN $CO_2$ (mM) | Ref. pH | Ref. $CO_3^{2-}$ ($\mu mol\,L^{-1}$) | Ref. $CO_2$ (mM) | Complete comparison |
|---|---|---|---|---|---|---|---|---|---|
| 1 | 7.96 | 200 | 8.05 | 247.3 | 0.5 | 8.00 | ND | $< 0.2$ | No |
| 2 | 7.72 | 90 | 7.72 | 59.3 | 0.8 | 7.73 | 72.1 | 0.8 | Yes |
| 3 | 7.71 | 90 | 7.69 | 80.9 | 1.2 | 7.78 | 90.9 | 1.0 | Yes |
| 4 | 7.35 | 50 | 7.43 | 49.6 | 2.4 | 7.51 | 58.1 | 2.3 | Yes |
| 5 | 7.04 | 10 | 6.94 | 8.8 | 4.1 | 7.03 | 10.2 | 3.5 | Yes |
| 6 | 6.95 | 10 | 7.03 | 2.1 | 6.2 | ND | ND | ND | No |

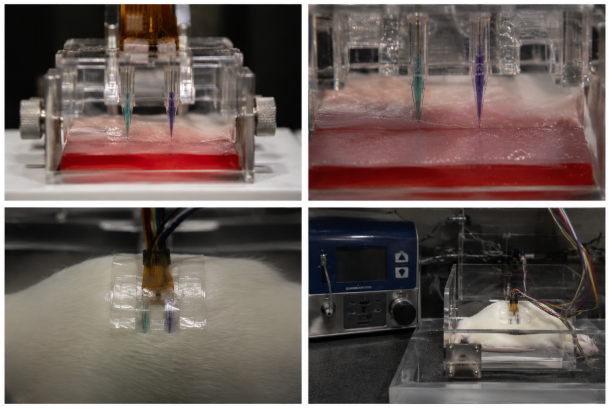

**Figure 5:** Skin-chamber measurement.

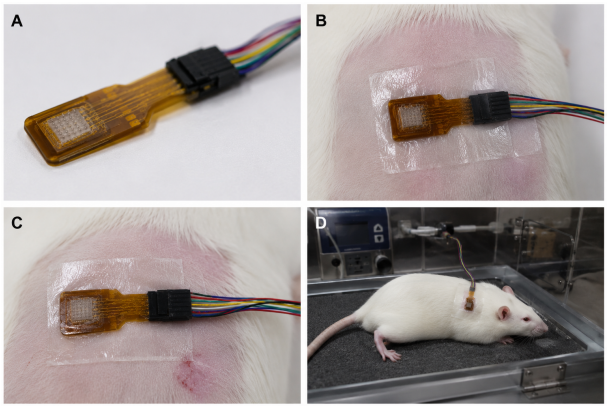


**Figure 6:** Patch placement sequence.

tion should occur if carbonate, bicarbonate, and transformed $PCO_2$ all suggest that the acid-base pair does not support blood proximity anymore. The distinction is crucial for KG-ABF since the pH reading could still be locally valid despite invalid estimates of carbon dioxide levels.

### 3.2. In vivo temporal measurements and gating results

The in vivo stage in Table 2 includes repetitive intradermal readings obtained from five rats. Rats 1, 2, and 3 were left with accepted readings at 15, 25, and 35 minutes. Rat 5 was left with accepted readings at 25 and 35 minutes. Rat 4 had a single accepted reading at 35 minutes but was rejected by the carbonate gate. The accepted rats included terminal blood-gas $PCO_2$ values between 18.8 mmHg and 53.7 mmHg.

It is evident that intradermal $PCO_2$ does not constitute a pool of interchangeable replicates based on the following observations. For rat 1, intradermal $PCO_2$ decreased from 18.8 mmHg at 25 min to 10.5 mmHg at 35 min despite its terminal blood level being at 18.8 mmHg. The level of intradermal $PCO_2$ for rat 2 stayed relatively high and was closer to the blood level throughout the process. Intradermal $PCO_2$ for rat 3 displayed the highest transitory peak at 25 min (73.6 mmHg) before falling back down to 41.2 mmHg at 35 min. Rat 5 had the smallest variability during the process. This justifies temporal sensitivity in merging data rather than treating each accepted value as a replicate.

The sequence of patch animal placement in Figure 6 shows how the numerical data correspond with the physical process. Handling of patches, skin contact,

It is clear from the staging views that the analytical data was collected while maintaining patch contact, rather than via separate insertions of single patches. This favors fusion within the animal, since the 15, 25, and 35 min entries represent a temporal progression based on one type of contact geometry.

The measurement station depicted in Figure 7 illustrates the cabled patch and positioning in the animal at acquisition time. Such a setup helps to clarify why the last reading point corresponds most directly to terminal blood gas values, although previous readings may still provide valid trajectories.

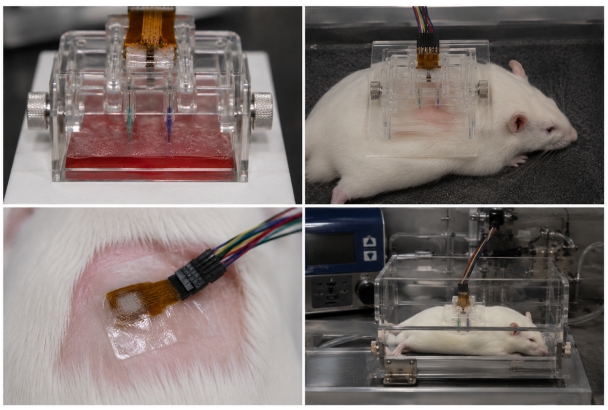

**Figure 7:** In vivo recording station.

The depiction of the measurement station emphasizes the temporal nature of the experimental procedure. Intradermal readings have been taken from an ongoing experiment and are to be correlated to a terminal blood gas measurement. As such, time is considered an integral part of the analytical process in KG-ABF.

The animal monitoring views illustrated in Figure 8 demonstrate repeat contact and chamber setups. While these are not quantitative measurements per se, they serve to explain why local variables may affect the variability between observations at different times in animals.

The figure demonstrates a careful evaluation of rat-specific variability. Positioning, exposure of the skin area, environment within the chamber, and wire handling may affect the stability of the intradermal

**Table 2:** In vivo records.

| Rat | Patch/time (min) | ISF pH | ISF $CO_3^{2-}$ ($\mu mol\,L^{-1}$) | ISF $HCO_3^-$ (mM) | ISF $CO_2$ (mM) | ISF $PCO_2$ (mmHg) | Gate |
|---|---|---|---|---|---|---|---|
| 1 | 1/15 | $7.52 \pm 0.02$ | $23.0 \pm 0.7$ | $10.8 \pm 0.5$ | $0.5 \pm 0.04$ | $17.3 \pm 1.3$ | accept |
| 1 | 2/25 | $7.61 \pm 0.07$ | $45.1 \pm 0.9$ | $18.3 \pm 0.1$ | $0.6 \pm 0.1$ | $18.8 \pm 2.3$ | accept |
| 1 | 3/35 | $7.78 \pm 0.12$ | $138.2 \pm 0.3$ | $18.6 \pm 0.8$ | $0.5 \pm 0.1$ | $10.5 \pm 1.9$ | accept |
| 2 | 4/15 | $7.27 \pm 0.05$ | $21.3 \pm 1.3$ | $25.3 \pm 0.9$ | $1.4 \pm 0.1$ | $45.8 \pm 4.3$ | accept |
| 2 | 5/25 | $7.17 \pm 0.04$ | $16.1 \pm 0.3$ | $22.0 \pm 1.6$ | $1.6 \pm 0.3$ | $62.5 \pm 0.6$ | accept |
| 2 | 6/35 | $7.24 \pm 0.02$ | $18.6 \pm 0.4$ | $20.7 \pm 1.1$ | $1.4 \pm 0.1$ | $49.8 \pm 1.9$ | accept |
| 3 | 7/15 | $7.39 \pm 0.03$ | $28.8 \pm 2.2$ | $23.3 \pm 0.9$ | $1.2 \pm 0.8$ | $39.3 \pm 2.5$ | accept |
| 3 | 8/25 | $7.17 \pm 0.04$ | $30.6 \pm 1.9$ | $23.3 \pm 3.9$ | $2.2 \pm 0.3$ | $73.6 \pm 9.7$ | accept |
| 3 | 9/35 | $7.33 \pm 0.02$ | $22.8 \pm 0.8$ | $21.1 \pm 0.5$ | $1.2 \pm 0.02$ | $41.2 \pm 0.7$ | accept |
| 4 | 10/35 | $7.21 \pm 0.13$ | $2.8 \pm 0.8$ | $2.9 \pm 0.5$ | $0.2 \pm 0.02$ | $7.5 \pm 0.6$ | reject |
| 5 | 11/25 | $7.22 \pm 0.18$ | $22.6 \pm 0.2$ | $13.1 \pm 0.8$ | $0.9 \pm 0.02$ | $29.8 \pm 0.5$ | accept |
| 5 | 12/35 | $7.56 \pm 0.02$ | $45.1 \pm 0.02$ | $18.3 \pm 0.4$ | $0.7 \pm 0.02$ | $25.4 \pm 0.7$ | accept |

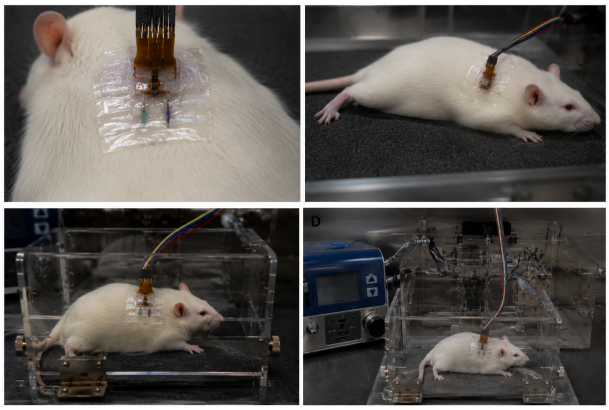

**Figure 8:** Monitoring views.

contact irrespective of sensor attachment. In this case, the use of a carbonate gate and spread descriptor becomes more reasonable than a sole numerical value outside of context.

Further views of the experimental animals are shown in Figure 9. The analysis of terminal blood values becomes more meaningful as part of the last values measured following an intradermal measurement series.

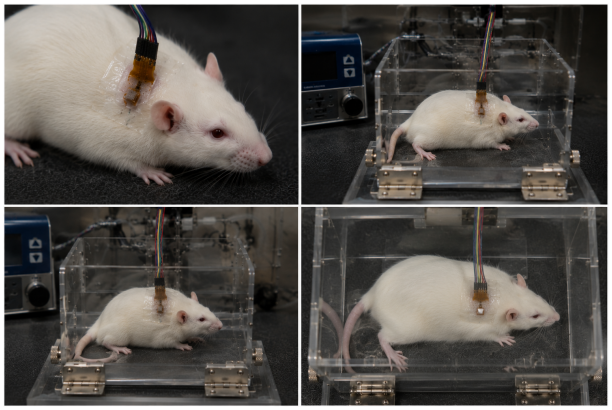

**Figure 9:** Terminal-period views.

The late-phase images further justify the weighting factor applied due to closeness to the blood sample. This does not necessarily mean the physiological synchronization, but shows that the intradermal series and late-phase blood-gas data are part of the same experimental process.

Details of the patch and chamber presented in Figure 10 are especially useful in the case of rat number 4, since visible attachment itself does not ensure a reportable carbonate condition. Consistency of chemistry should be demonstrated using pH-carbonate data.

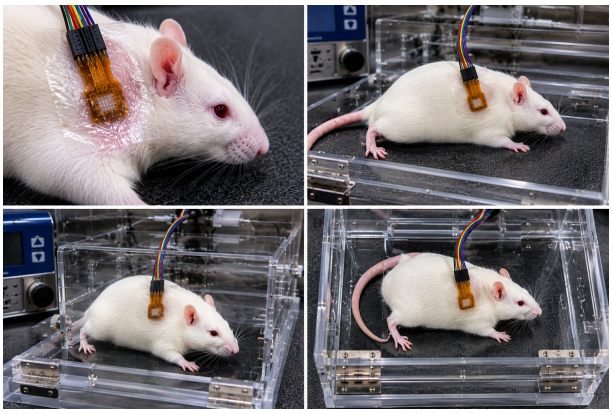

**Figure 10:** Patch and chamber details.

The carbonic acid levels measured in Rat 4 were $2.8\,\mu mol\,L^{-1}$, bicarbonate $2.9\,mmol\,L^{-1}$, and skin blood partial pressure of carbon dioxide ($PCO_2$) 7.5 mmHg. Blood gas parameters in terms of the terminal blood gas for the same animal were blood pH 7.5, bicarbonate $27.6\,mmol\,L^{-1}$, and $PCO_2$ 23.9 mmHg. This difference cannot be considered a trivial numerical variation but a chemical impossibility for blood-proximal assignment. Accordingly, rejection will be based on a predefined criterion, not ad hoc exclusion of a problematic point.

### 3.3. Animal-level agreement with terminal blood gas

Based on the results of quality gating, Table 3 presents the animal-level estimation results. There were four animals meeting the criteria for blood-proximal assignment. Their KG-ABF errors varied between $-4.1$ mmHg to 4.2 mmHg, giving a mean absolute error of 3.1 mmHg, a root-mean-square error of 3.3 mmHg, and a maximum absolute error of 4.2 mmHg. Every accepted estimate fell inside the prespecified 7.5 mmHg agreement band.

The spread descriptor provides information that the error cannot. Rat 3's error was very low at only $-2.5$ mmHg, yet its spread descriptor was quite high at 16.4 mmHg, much larger than that of rat 5. In

**Table 3:** Animal-level agreement.

| Rat | Accepted times (min) | Blood pH | Blood $HCO_3^-$ (mM) | KG-ABF estimate (mmHg) | Spread descriptor (mmHg) | Blood $PCO_2$ (mmHg) | Error (mmHg) |
|---|---|---|---|---|---|---|---|
| 1 | 15, 25, 35 | 7.7 | 23.1 | 14.7 | 4.3 | 18.8 | -4.1 |
| 2 | 15, 25, 35 | 7.3 | 14.0 | 53.0 | 7.2 | 48.8 | 4.2 |
| 3 | 15, 25, 35 | 7.4 | 29.8 | 51.2 | 16.4 | 53.7 | -2.5 |
| 4 | none after gate | 7.5 | 27.6 | – | – | 23.9 | excluded |
| 5 | 25, 35 | 7.6 | 25.7 | 27.2 | 2.3 | 25.4 | 1.8 |

spite of the instability of the intradermal trajectory, the animal-level estimate did agree with blood gas due to this additional information. This differentiation in a wearable instrument could enable separate representation of the numerical value and its reliability.

Agreement panels in Figure 11 present three different ways of interpreting the accepted records: unweighted average considers all of them equally valid, the last reading considers only the value at 35 min, while KG-ABF uses both approaches together.

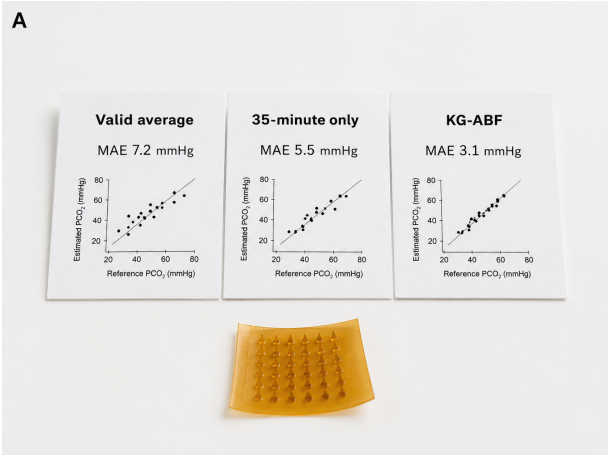


**Figure 11:** Agreement panels.

The comparison in Figure 11 illustrates that the gain is due to the chemical analysis of the same sensor measurements and not to changes in those sensor measurements themselves. This is significant for development of analytical methods because KG-ABF improves the information content of decisions through better chemistry and timing.

Error comparison in Figure 12 summarizes the results for all three methods into one graph. As would be expected from the tabulated results, the highest errors were seen in the unweighted average, the next lowest was achieved with the terminal-only method, and the best result came from KG-ABF.

The decrease from 7.2 mmHg mean absolute error when taking averages of valid measurements without weighting to 3.1 mmHg when applying KG-ABF algorithm is of great significance since there were no extra blood samples nor extra sensor channels added. This improvement was achieved by simply acknowledging that a time-series intradermal measurement cannot be simplified into an arithmetic average and that depleted measurements need not conform to a blood-near measurement.

The sheet labeled as 'Accepted Animals' in Figure 13 shows the final set of animals after excluding rat 4 through the carbonate gate.

This conclusion is reinforced in the final diagram, showing that KG-ABF does more than minimize error; it also specifies eligibility of data points for inclusion, contribution of accepted time points, and residual variability per animal path.

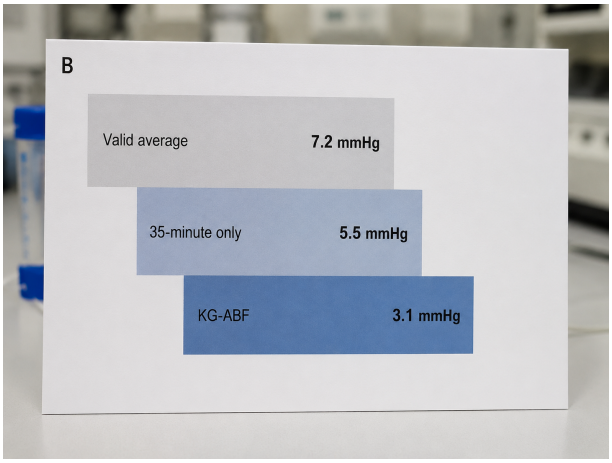


**Figure 12:** Error comparison.

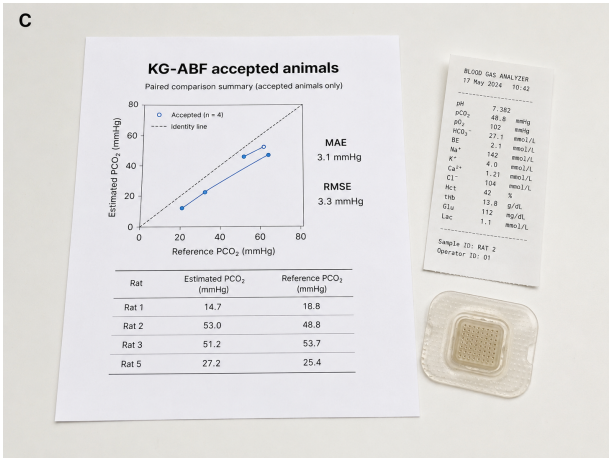


**Figure 13:** Accepted-animal summary.

### 3.4. Interpretation of animal-specific behavior

For example, rat 1 shows that a measurement taken at the end of an experiment alone cannot fully capture the phenomenon being measured. The 35 min measurement from the intradermal point was less than the terminal value from the blood-gas measurement point, and the 25 min measurement was close to the blood-gas measurement. KG-ABF adjusted for this final small number by incorporating the early measurements that had been accepted, obtaining 14.7 mmHg, an error of −4.1 mmHg.

Rat 2 shows steady elevation instead of single drift. All accepted intradermal measurements showed elevated levels of carbon dioxide, and the 35 min level of 49.8 mmHg approached the blood measurement of 48.8 mmHg. For this rat, KG-ABF returned 53.0 mmHg, which was somewhat greater than blood measurement but still with very small

errors. Thus, this procedure may classify an animal as high-$PCO_2$ one even if some values appear to be false sensor readings.

Rat 3 turned out to be the most temporally variable among all the accepted animals. In the middle of its intradermal time series, the level of 73.6 mmHg could skew the average calculation, whereas using only the final measurement might underestimate terminal blood measurement. However, the KG-ABF method made an adequate compromise between two extremes and gave 51.2 mmHg, contrasting with 53.7 mmHg for blood measurement. The description with the

For rat 5, there were two accepted readings and the smallest spread descriptor. With the KG-ABF estimate of 27.2 mmHg, we are near the value from the blood-gas reading of 25.4 mmHg. This particular instance is evidence of how the fusion rule can function with a shortened accepted series as long as chemistry still qualifies as a candidate and terminal proximity weighting still holds.

The instance for rat 4 asks a different question regarding analysis: Is it appropriate to allocate a numerical value even when chemistry does not allow blood-proximal interpretation? In KG-ABF's case, the answer is no. This particular instance was not excluded on account of statistical inconvenience but on the basis of chemical impracticality, as carbonate, bicarbonate, and transformed intradermal $PCO_2$ are lower than any practical chemistry limit while the corresponding blood-gas values do not share this property.

### 3.5. Significance and limitations of analysis

The most significant analytical insight provided by the KG-ABF approach is the generation of a response to the pH–carbonate microneedle pairing in terms of three specific outcomes: chemical feasibility, an $PCO_2$ value for blood proximal to the animal when acceptability criteria have been met, and a dispersion parameter that describes intra-animal variability. This form of analysis provides better compatibility with the data acquisition process due to consideration of working range issues and the temporal context in which measurements were made.

Another benefit offered by the approach relates to its recognition of the chemical significance of the microneedles used to acquire the carbon dioxide data. The carbonate response does not simply act as a supplement, but is necessary to determine whether a transformed value for carbon dioxide concentration is a chemically plausible result. This understanding of the process follows from a general knowledge of ion-selective electrode theory, wherein the membrane characteristics, working range, and activity effects are responsible for determining validity of the resulting measured concentrations [13, 14, 17].

The first limitation is due to the small sample size. There were only five subjects to conduct in vivo experiments on, and one subject contributed to only a single data point that did not meet the eligibility criteria. The blood gas was measured after death, but not synchronously with each intradermal time point. The gate limit values were determined analytically here, and they cannot simply be applied prospectively to humans in similar ways without experimental verification. It needs to be tested further in larger populations of animals and humans with various temperatures, ventilation statuses, locations, and manufacturing batch variations.

Another limitation was that bicarbonate levels were assumed based on their relation to the acid-base condition instead of being directly measured with a bicarbonate selective microneedle. A better designed patch could incorporate additional features such as bicarbonate measurement, temperature calibration, diagnostics for the reference electrode, and monitoring of hydration state, as well as automatic flagging of equilibration instability. In future experiments, the KG-ABF measurement should be compared directly to measurements made simultaneously with arterial or venous blood gas sampling.

## 4. Conclusion

The research question in this study was whether a combination of carbonate gating and terminal-proximity fusion can enhance blood-proximal carbon dioxide inference in the paired intradermal pH-carbonate microneedle data. The result is affirmative for the examined rat skin and anesthetized rat record. KG-ABF preserved eligible chemical observations, omitted the rat 4 observation due to its carbonate deficiency, and yielded a mean absolute error of 3.1 mmHg with respect to the terminal blood-gas $PCO_2$. The root-mean-square error obtained by KG-ABF was 3.3 mmHg, with the maximum absolute error being 4.2 mmHg. All accepted observations were located within the 7.5 mmHg agreement band. The enhanced accuracy of KG-ABF compared to the simple unweighted average or final reading inference occurred because of the selective utilization of the available measurements rather than additional channel information or blood sampling. In particular, the exclusion of the rat 4 observation is critical for the overall result, since a valid intradermal carbon dioxide test needs to be able to refuse assignments to a blood-proximal value.

## Data Availability

All numerical values evaluated in the analysis are shown in Tables 1, 2, and 3. The visual documentation supporting the experimental context is provided in Figures 1–13.

## Ethical Statement

No separate animal experiments were conducted for this analysis. The animal-related values are the rat-skin, intradermal microneedle, and terminal blood-gas measurements listed in the manuscript tables.

## Conflict of Interest

The author declares no conflict of interest.

## References

[1] Severinghaus, J. W., & Bradley, A. F. (1958). Electrodes for blood $pO_2$ and $pCO_2$ determination. *Journal of Applied Physiology*, *13*(3), 515–520.
[2] Eberhard, P. (2007). The design, use, and results of transcutaneous carbon dioxide analysis: Current and future directions. *Anesthesia & Analgesia*, *105*(6), S48–S52.
[3] Conway, A., Tipton, E., Liu, W. H., Conway, Z., Soalheira, K., Sutherland, J., & Fingleton, J. (2019). Accuracy and precision of transcutaneous carbon dioxide monitoring: A systematic review and meta-analysis. *Thorax*, *74*(2), 157–163.
[4] Heikenfeld, J., Jajack, A., Rogers, J., Gutruf, P., Tian, L., Pan, T., ... & Wang, J. (2018). Wearable sensors: Modalities, challenges, and prospects. *Lab on a Chip*, *18*(2), 217–248.
[5] Friedel, M., Thompson, I. A., Kasting, G., Polsky, R., Cunningham, D., Soh, H. T., & Heikenfeld, J. (2023). Opportunities and challenges in the diagnostic utility of dermal interstitial fluid. *Nature Biomedical Engineering*, *7*(12), 1541–1555.
[6] Bandodkar, A. J., & Wang, J. (2014). Non-invasive wearable electrochemical sensors: A review. *Trends in Biotechnology*, *32*(7), 363–371.
[7] Gao, W., Emaminejad, S., Nyein, H. Y. Y., Challa, S., Chen, K., Peck, A., ... & Javey, A. (2016). Fully integrated wearable sensor arrays for multiplexed in situ perspiration analysis. *Nature*, *529*(7587), 509–514.
[8] Henry, S., McAllister, D. V., Allen, M. G., & Prausnitz, M. R. (1998). Microfabricated microneedles: A novel approach to transdermal drug delivery. *Journal of Pharmaceutical Sciences*, *87*(8), 922–925.
[9] Prausnitz, M. R. (2004). Microneedles for transdermal drug delivery. *Advanced Drug Delivery Reviews*, *56*(5), 581–587.
[10] Parrilla, M., Cuartero, M., Padrell Sánchez, S., Rajabi, M., Roxhed, N., Niklaus, F., & Crespo, G. A. (2018). Wearable all-solid-state potentiometric microneedle patch for intradermal potassium detection. *Analytical Chemistry*, *91*(2), 1578–1586.

[11] García-Guzmán, J. J., Pérez-Ràfols, C., Cuartero, M., & Crespo, G. A. (2021). Toward in vivo transdermal pH sensing with a validated microneedle membrane electrode. *ACS Sensors*, *6*(3), 1129–1137.
[12] Molinero-Fernandez, A., Casanova, A., Wang, Q., Cuartero, M., & Crespo, G. A. (2022). In vivo transdermal multi-ion monitoring with a potentiometric microneedle-based sensor patch. *ACS Sensors*, *8*(1), 158–166.
[13] Bakker, E., Pretsch, E., & Bühlmann, P. (2000). Selectivity of potentiometric ion sensors. *Analytical Chemistry*, *72*(6), 1127–1133.
[14] Bühlmann, P., Pretsch, E., & Bakker, E. (1998). Carrier-based ion-selective electrodes and bulk optodes. 2. Ionophores for potentiometric and optical sensors. *Chemical Reviews*, *98*(4), 1593–1688.
[15] Umezawa, Y., Buhlmann, P., Umezawa, K., Tohda, K., & Amemiya, S. (2000). Potentiometric selectivity coefficients of ion-selective electrodes. Part I. Inorganic cations. *Pure and Applied Chemistry*, *72*(10), 1851–2082.
[16] Molinero-Fernandez, Á., Wang, Q., Xuan, X., Konradsson-Geuken, Å., Crespo, G. A., & Cuartero, M. (2024). Demonstrating the analytical potential of a wearable microneedle-based device for intradermal $CO_2$ detection. *ACS Sensors*, *9*(1), 361–370.
[17] Wilson, G. S., Buck, R. P., Rondinini, S., Covington, A. K., Baucke, F. G. K., Brett, C. M. A., ... & Spitzer, P. (2002). Measurement of pH: Definition, standards, and procedures.